Journal of Materials and Environmental Sciences
ISSN : 2028-2508
CODEN : JMESCN

JMES, 2017 Volume 8, Issue 11, Page 3844-3854

http://www.jmaterenvironsci.com /

Synthesis, physicochemical, conformation and quantum calculation of novel N-(1-(4-bromothiophen-2-yl)ethylidene)-2-(piperazin-1-yl)ethanamine Schiff base

Ismail Warad[1]*, Oraib Ali[1], Riham Ahed[1], Abdallah Bani Odeh[2], Sameer A. Barghouthi[2] Shivalingegowda Naveen[3], Hicham Elmsellem[4], Iqab Daraghmeh[5] Lokanath N. K.[6], Mustapha Allali[7]

[1]*Department of Chemistry, AN-Najah National University P.O. Box 7, Nablus, Palestine*
[2]*Departement of medical laboratory sciences, Al Quds University, Jerusalem, Palestine*
[3]*Institution of Excellence, Vijnana Bhavana, University of Mysore, Manasagangotri, Mysuru 570 006, India*
[4] *LC2AME, Faculty of Science, First Mohammed University, PO Box 717, 60 000 Oujda, Morocco.*
[5]*Department of Chemistry, Arab American University-Jenin, P.O. Box, Jenin, Palestine*
[6]*Department of Studies in Physics, University of Mysore, Manasagangotri, Mysore - 570 006, India*
[7]*Institut Supérieur des Professions Infirmières et Techniques de Santé, ISPITS De Fès, Morocco.*

Received 22 May 2017,
Revised 18 Jun 2017,
Accepted 21 Jun 2017

Keywords
- ✓ Schiff base,
- ✓ NMR,
- ✓ DFT,
- ✓ Conformational,
- ✓ Spectral.

warad@najah.edu
Phone: 009709234003;
Fax: 0097092345982

Abstract

N-(1-(4-bromothiophen-2-yl)ethylidene)-2-(piperazin-1-yl)ethanamine Schiff base ligand was prepared in very good yield by condensation of equimolar amounts of 1-(4-bromothiophen-2-yl)ethanone with 2-(piperazin-1-yl)ethanamine under reflux condition using alcohol media. The desired Schiff base was analyzed on the basis of its MS, elemental analysis, UV-visible, FT-IR and NMR analysis. The E and Z optimization was performed to figure out the most stable isomer. Several DFT quantum calculation like: TD-SCF, MPE, IR-vibration, NMR, Mulliken population were carried out by B3LYP level of theory. The experimental analyses of the compound were compared to their theoretical coordinates.

1. Introduction

The azomethine group (>C=N-) distinguishes the Schiff base (S.B.) compounds which was announced first by Hugo Schiff in 1864 and prepared through condensation of primary amine with carbonyls (with and without acid or base catalyst) under reflux using ROH solvent [1]. S.B molecules are wonderful chelators due to their electrons free availability, freedom in design, ease of synthesis, simple in analysis, stability and structural varieties [2]. S.B ligands have main unsaturated N-potential sites with open possibility of other donor atoms like O, S, P or any atoms with free pair of electros; accordingly, it can be considered as prerogative metal ions ligands [3]. S.B compounds are very remarkable material especially for inorganic people, as these are openly applied in complexation and coordination filed of research, it generated as an excellent mono- or poly dentate ligand [4]. S.B and their complexes were used in medicinal inorganic field due to their diverse pharmacological, biological and antitumor effectiveness [3, 4].

Schiff-bases acquired much significance in designing, modeling, magnet molecules applications, and in crystals filed [5]. In general, several medical applications like antioxidant, antifungal, antibacterial, anti-inflammatory, antitumor, and antipyretic have been evaluated [6-11]. S.B in industry used as catalysts, polymer stabilizers, pigments, and anti-corrosion agent [12-16].

In correlation with our research in Schiff bases synthesis and their complexation as well as their biological applications [14-23], here in this work, N-(1-(4-bromothiophen-2-yl)ethylidene)-2-(piperazin-1-yl)ethanamine was prepared and characterized by several available spectral analysis. Several quantum calculations like: DFT

optimization structure of both *E* and *Z* forms, MPE, Mulliken population, NMR, TD-DFT, UV-Visible were carried out and compared to the experiential analysis.

2. Experimental

2.1. General

All the Martials used were purchased from Sigma, EA was carried out on an Elementar-Vario EL analyzer; FT-IR spectra were recorded on a Perkin-Elmer Spectrum-Spectrometer as KBr pellets, whereas UV-Visible spectra obtained with a TU-1901- UV–visible spectrophotometer. NMR spectra were acquired on Bruker DRX 500 using TMS as the internal standard and $CDCl_3$ as solvent.

2.2. Synthesis of S.B.

The desired S.B compound was produced by mixing 1-(4-bromothiophen-2-yl)ethanone (10 mmol) in 10 ml MeOH with 10 mmol of 2-(piperazin-1-yl)ethanamine in 10 ml MeOH, the mixture was subjected vigorous reflux for 4 hours. White powder was obtained after slow evaporation of MeOH solvent, which was washed several times with n-hexane, then dried under vacuum, Yield 82%.

2.3. Computational analysis

QM calculations and *E-Z* isomers optimization of the desired S.B was performed using the GAUSSIAN09 with DFT/B3LYP-6-31G(d) basis set [28].

3. Results and discussion

Synthesis

The N-(1-(4-bromothiophen-2-yl)ethylidene)-2-(piperazin-1-yl)ethanamine ligand was prepared by condensation of equimolar amounts of 2-(piperazin-1-yl)ethanamine with 1-(4-bromothiophen-2-yl)ethanone in methanol under reflux condition for 4h, as shown in Scheme 1. The product which was collected at the end of the reaction after methanol evaporation was washed with *n*-hexane, non-soluble impurities were filtrated out. The structure of the desired S.B product was investigated by several spectroscopic techniques such as: ^{1}H-NMR, FT-IR, and UV-visible in addition to MS and elemental analyses. The S. B was also subjected to several quantum calculations such: optimization, *E-Z* conformation, TD-SCF, MPE, IR-vibration, estimated-NMR and Mulliken population.

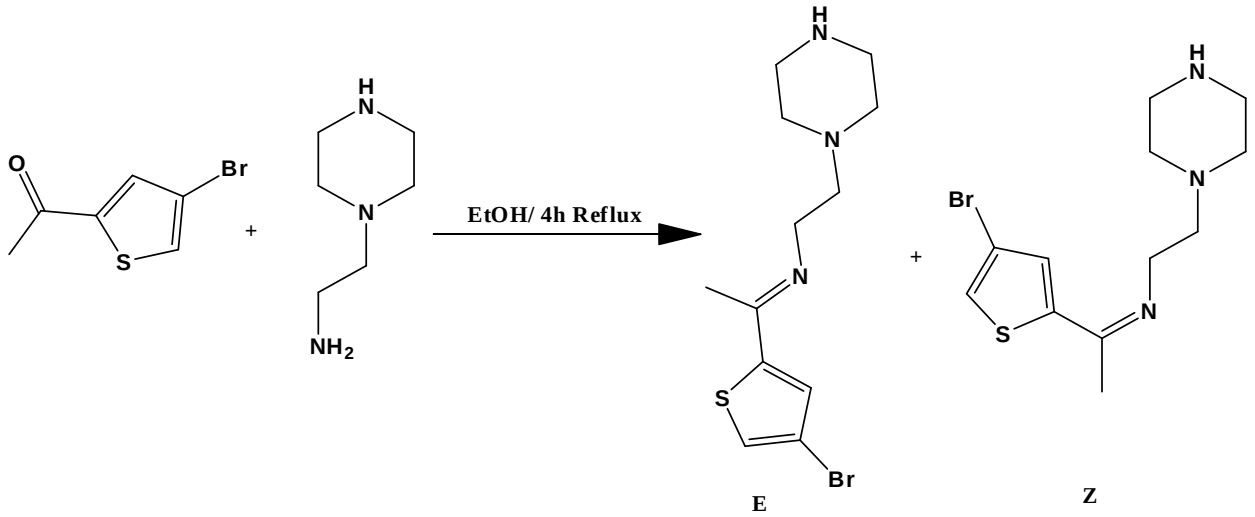

***N*-(1-(4-bromothiophen-2-yl)ethylidene)-2-(piperazin-1-yl)ethanamine**

Scheme 1. *Synthesis of desired S.B.*
E-Z conformational optimization.

The molecular structure geometries of the *E* and *Z* isomers belong to the synthesized S. B. compound was optimized in gaseous state at DFT/B3LYP6-31G(d) level of theory. The optimized structures are illustrated in Fig. 1; some optimized parameters are listed in Table 1.

Table 1. Calculated total energy of *E* and *Z* isomers of the S.B.

DFT/B3LYP 6-31G(d)	E	Z
Total Energy in Hartree	-3602.21851403	-3602.21585894
Dipole Moment in Debye	1.6631	2.0132
Point Group	C1	C1
$E_z > E_E$, ΔE = 6.98 kJ/mol		

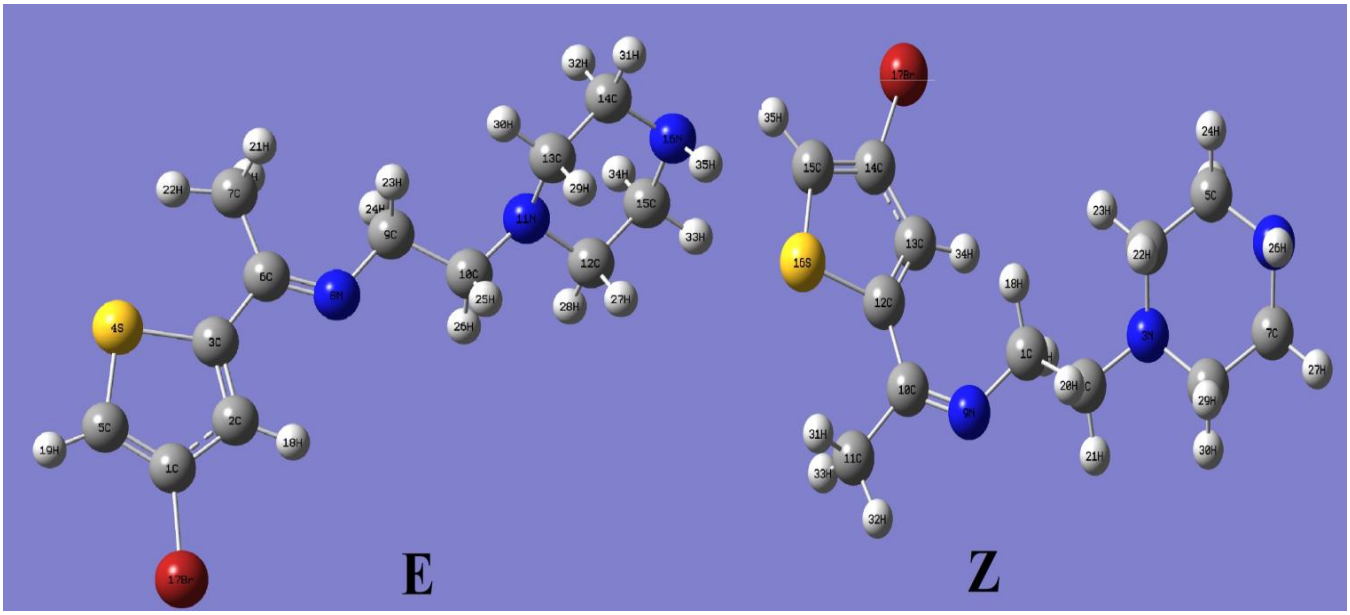

Fig. 1. Ground state optimization geometries of *E* and *Z* isomer of the desired S. B at B3LYP/6-31G(d) levels of theory**.**

It was observed from Fig. 1 and Scheme 1 that the steric hindrance caused by thiophene ring and CH_2-CH_2-piperizene around C=N in *Z*-isomer (syn-form) raises the energy of such isomer compared to *E*-isomer (anti-form). Such observation reflects the preference of dominating *E*-isomer.
The DFT theoretical calculations in the gas phase is consistent with result, the *E*-isomer (-3602.21851403 a.u.) is the more stable than *Z*-isomer (-3602.21585894 a.u.) since its total energy calculated found to be less than *Z* form, as see Table 1.

The theoretical calculation focused on the placement of rotational barriers from the *Z* to *E*-isomers. The proportional *Z*-*E* conformers energies (Fig. 1), obtained by rotating CH_2-CH_2-piperizene around the C=N bond in *E* anti-form to reach the Z syn-form of about 124^o. The computed energy minima of both isomers corresponding to -$C_{theophine}$-C=N-CH_2- torsion angle, the corresponding torsion angle in *E* found to be 179.8^o whereas for Z-isomer equal 3.1^o. The barrier energy relying on the direction of the rotation from anti to syn-forms is about 7 kJ/mol, which is a very small rotational energy, as see Table 1.

E-isomer optimization structural parameters
Because E-isomer of the desired ligand found to be more stable than Z-isomer, the optimization geometric parameters of it only are illustrated in Tables 2-3. The structural parameters like bond lengths (Tables 2), angles (Tables 3), and dihedral angles (Tables 3) were performed on B3LYP/6-31G(d) level of theory.

Table 2. B3LYP/6-31G(d) calculated bond lengths values (Å).

Bond No.	Bond type		DFT/B3LYP 6-31G(d)	No. Bond	Bond type		DFT/ B3LYP 6-31G(d)
1	C1	C2	1.4185	19	C10	N11	1.4611
2	C1	C5	1.3679	20	C10	H25	1.1071
3	C1	Br17	1.8989	21	C10	H26	1.0958
4	C2	C3	1.3754	22	N11	C12	1.465
5	C2	H18	1.0817	23	N11	C13	1.4649
6	C3	S4	1.7543	24	C12	C15	1.534
7	C3	C6	1.477	25	C12	H27	1.1115
8	S4	C5	1.7298	26	C12	H28	1.0971
9	C5	H19	1.0805	27	C13	C14	1.535
10	C6	C7	1.5175	28	C13	H29	1.1118
11	C6	N8	1.282	29	C13	H30	1.0961
12	C7	H20	1.0966	30	C14	N16	1.4653
13	C7	H21	1.0969	31	C14	H31	1.0963
14	C7	H22	1.0922	32	C14	H32	1.0977
15	N8	C9	1.4548	33	C15	N16	1.4661
16	C9	C10	1.5326	34	C15	H33	1.0962
17	C9	H23	1.1013	35	C15	H34	1.0977
18	C9	H24	1.1013	36	N16	H35	1.0209

Table 3. B3LYP/6-31G(d) calculated angles values (^{o}).

Angle No.	Angles types			DFT/B3LYP 6-31G(d)	Angle No.	Angles types			DFT/B3LYP 6-31G(d)
1	C2	C1	C5	114.31	34	N11	C10	H26	108.17
2	C2	C1	Br17	122.74	35	H25	C10	H26	106.46
3	C5	C1	Br17	122.96	36	C10	N11	C12	112.1
4	C1	C2	C3	112.52	37	C10	N11	C13	112.94
5	C1	C2	H18	124.91	38	C12	N11	C13	110.34
6	C3	C2	H18	122.57	39	N11	C12	C15	110.52
7	C2	C3	S4	110.49	40	N11	C12	H27	111.51
8	C2	C3	C6	126.56	41	N11	C12	H28	108.54
9	S4	C3	C6	122.95	42	C15	C12	H27	109.14
10	C3	S4	C5	92.1	43	C15	C12	H28	109.98
11	C1	C5	S4	110.58	44	H27	C12	H28	107.08
12	C1	C5	H19	128.41	45	N11	C13	C14	110.54
13	S4	C5	H19	121.02	46	N11	C13	H29	111.07
14	C3	C6	C7	119.38	47	N11	C13	H30	109.38
15	C3	C6	N8	116.38	48	C14	C13	H29	109.34
16	C7	C6	N8	124.23	49	C14	C13	H30	109.5
17	C6	C7	H20	110.22	50	H29	C13	H30	106.94
18	C6	C7	H21	110.22	51	C13	C14	N16	113.7
19	C6	C7	H22	113.43	52	C13	C14	H31	110
20	H20	C7	H21	106.91	53	C13	C14	H32	108.77
21	H20	C7	H22	107.9	54	N16	C14	H31	108.86
22	H21	C7	H22	107.91	55	N16	C14	H32	107.75
23	C6	N8	C9	119.85	56	H31	C14	H32	107.57
24	N8	C9	C10	109.14	57	C12	C15	N16	113.59
25	N8	C9	H23	110.17	58	C12	C15	H33	110.08
26	N8	C9	H24	111.97	59	C12	C15	H34	108.8
27	C10	C9	H23	110.74	60	N16	C15	H33	108.86
28	C10	C9	H24	108.56	61	N16	C15	H34	107.74
29	H23	C9	H24	106.23	62	H33	C15	H34	107.58
30	C9	C10	N11	112.94	63	C14	N16	C15	110.34
31	C9	C10	H25	109.17	64	C14	N16	H35	108.63
32	C9	C10	H26	107.38	65	C15	N16	H35	108.61
33	N11	C10	H25	112.38					

Table 4. B3LYP/6-31G(d) calculated dihedral angles values (°).

Angle No.	Angles type				DFT/B3LYP 6-31G(d)	Angle No.	Angles type				DFT/B3LYP 6-31G(d)
1	C5	C1	C2	C3	-0.03	45	H26	C10	N11	C12	-39.78
2	C5	C1	C2	H18	179.99	46	H26	C10	N11	C13	-165.18
3	Br17	C1	C2	C3	179.87	47	C10	N11	C12	C15	175.61
4	Br17	C1	C2	H18	-0.11	48	C10	N11	C12	H27	-62.8
5	C2	C1	C5	S4	0.02	49	C10	N11	C12	H28	54.92
6	C2	C1	C5	H19	179.96	50	C13	N11	C12	C15	-57.58
7	Br17	C1	C5	S4	-179.88	51	C13	N11	C12	H27	64.02
8	Br17	C1	C5	H19	0.07	52	C13	N11	C12	H28	-178.26
9	C1	C2	C3	S4	0.02	53	C10	N11	C13	C14	-176.28
10	C1	C2	C3	C6	179.96	54	C10	N11	C13	H29	62.17
11	H18	C2	C3	S4	-179.99	55	C10	N11	C13	H30	-55.64
12	H18	C2	C3	C6	-0.05	56	C12	N11	C13	C14	57.38
13	C2	C3	S4	C5	-0.01	57	C12	N11	C13	H29	-64.17
14	C6	C3	S4	C5	-179.96	58	C12	N11	C13	H30	178.02
15	C2	C3	C6	C7	179.57	59	N11	C12	C15	N16	55.28
16	C2	C3	C6	N8	-0.57	60	N11	C12	C15	H33	177.64
17	S4	C3	C6	C7	-0.49	61	N11	C12	C15	H34	-64.7
18	S4	C3	C6	N8	179.36	62	H27	C12	C15	N16	-67.7
19	C3	S4	C5	C1	0	63	H27	C12	C15	H33	54.65
20	C3	S4	C5	H19	-179.95	64	H27	C12	C15	H34	172.31
21	C3	C6	C7	H20	-122.63	65	H28	C12	C15	N16	175.11
22	C3	C6	C7	H21	119.6	66	H28	C12	C15	H33	-62.54
23	C3	C6	C7	H22	-1.52	67	H28	C12	C15	H34	55.12
24	N8	C6	C7	H20	57.52	68	N11	C13	C14	N16	-54.95
25	N8	C6	C7	H21	-60.25	69	N11	C13	C14	H31	-177.32
26	N8	C6	C7	H22	178.63	70	N11	C13	C14	H32	65.1
27	C3	C6	N8	C9	179.85	71	H29	C13	C14	N16	67.62
28	C7	C6	N8	C9	-0.3	72	H29	C13	C14	H31	-54.75
29	C6	N8	C9	C10	-175.84	73	H29	C13	C14	H32	-172.33
30	C6	N8	C9	H23	62.36	74	H30	C13	C14	N16	-175.51
31	C6	N8	C9	H24	-55.63	75	H30	C13	C14	H31	62.12
32	N8	C9	C10	N11	175.94	76	H30	C13	C14	H32	-55.46
33	N8	C9	C10	H25	-58.27	77	C13	C14	N16	C15	50.87
34	N8	C9	C10	H26	56.77	78	C13	C14	N16	H35	-68.08
35	H23	C9	C10	N11	-62.61	79	H31	C14	N16	C15	173.87
36	H23	C9	C10	H25	63.19	80	H31	C14	N16	H35	54.91
37	H23	C9	C10	H26	178.22	81	H32	C14	N16	C15	-69.76
38	H24	C9	C10	N11	53.65	82	H32	C14	N16	H35	171.29
39	H24	C9	C10	H25	179.44	83	C12	C15	N16	C14	-51.02
40	H24	C9	C10	H26	-65.52	84	C12	C15	N16	H35	67.95
41	C9	C10	N11	C12	-158.49	85	H33	C15	N16	C14	-174.05
42	C9	C10	N11	C13	76.11	86	H33	C15	N16	H35	-55.08
43	H25	C10	N11	C12	77.45	87	H34	C15	N16	C14	69.57
44	H25	C10	N11	C13	-47.95	88	H34	C15	N16	H35	-171.46

MS and elemental analyses

The experimental Ms and elemental analyses of the prepared S.B are consistent with it molecular formula $C_{12}H_{18}BrN_3S$, Calcd: C, 45.57; H, 5.74; N, 13.29; Found: C, 45.49; H, 5.61; N, 13.15), EI-MS experimental spectrum $[M^+]$ *m/z* = 316.0 (316.2 theoretical).

Theoretical ^1H NMR compared to experimental

The typical (experimental and theoretical) ^{1}H-NMR of the desired S.B is illustrated in Fig. 2, which showed a sharp broad signal at δ 1.50 ppm cited to NH proton, broad singlet peak corresponding to CH_3 group is detected at 2.02 ppm, two broad peaks at 2.45 and 2.55 ppm belongs to CH_2 of the piperzine, triplets signals at 2.90 and 3.55 ppm with J_{H-H} = 6.2 Hz were attributed to =N-CH_2-C$\underline{H_2}$-N and =N-C$\underline{H_2}$-CH_2-N, respectively. The C-H thiophene protons were detected as singles at *δ* 6.98 and 7.12 ppm, see Fig. 2a.

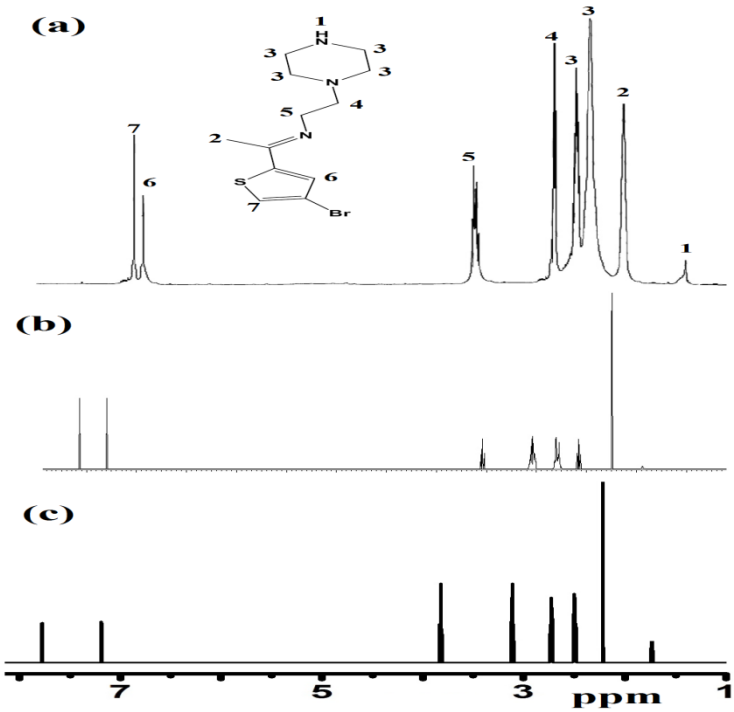

Fig. 2. ^{1}H NMR spectra of S.B. a) experimental in $CDCl_3$ at RT, b) ACD-LAB theoretical and c) NMR-DB theoretical

.

The ACD-LAB and NMR-DB [24] computed ^{1}H NMR result was illustrated in Fig. 2b and Fig.2c respectively. In general, Fig. 2. reflected an excellent chemical shifts correlation between experimental and computed ^{1}H NMR. The correlation coefficient (CC) values of chemical shifts resolved by ACD-LAB and NMR-DB versus experimental ^{1}H-NMR are 0.978 and 0.988, respectively.

FT-IR and DFT/B3LYP/6-31G(d)-IR

The FT-IR spectrum of the solid product showed a number of absorption bands related to its functional groups vibration, as seen in Fig. 3a. DFT-IR analysis for the same compound was computed at B3LYP/6-31G(d) level in the gaseous state, as seen in Fig. 3b.

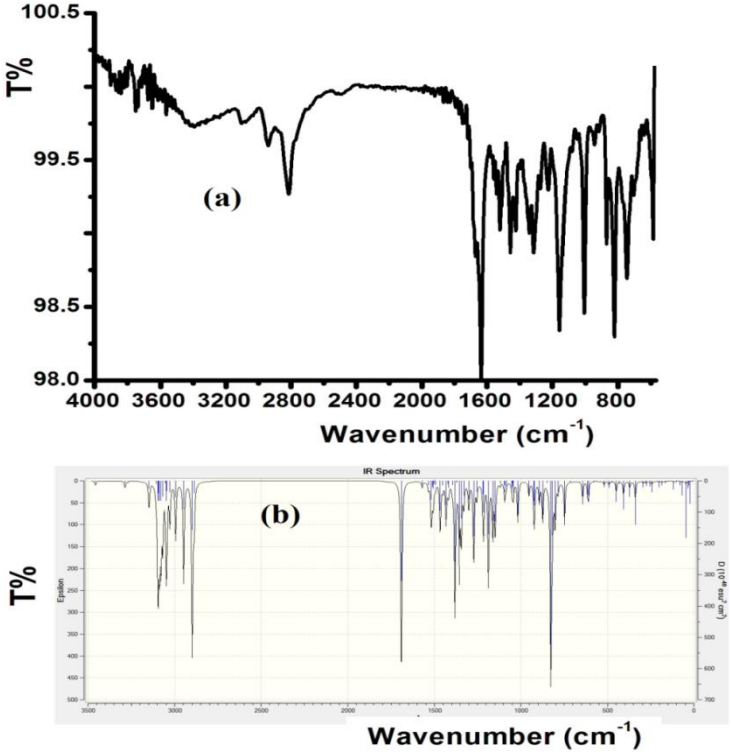

Fig. 3. (a) Experimental FT-IR spectrum of S.B and (b) theoretical vibration spectrum at DFT/B3LYP 6-31G(d).

The main experimental and theoretical stretching vibration bands are illustrated in Table 5. The theoretical and experimental FT-IR spectra revealed an acceptable agreement [14, 15].

Table 5. Calculated and experimental frequency vibrations of the main functional groups belong to S.B.

Approximate assignments	Experimental	B3LYP/6-31G(d)
N-H	3380	3420
C-H (thiophene and aliphatic)	3080-2860	3100-2860
C=N	1660	1680
C=C (thiophene)	1440-1590	1460-1600

There was a minor conflict, however, because the DFT- calculation was carried out in free gaseous state, whereas experimental was performed in solid state, the DFT-theoretical calculations expected to larger [25, 26].

UV-Visible and TD-DFT/B3LYP 6-31G(d)

The electronic absorption of the synthesised S.B was carried out in MeOH. Two signals were detected only in the UV region with λ_{max} = 255 nm and λ_{max} = 292 nm attributed to π-π* intra-ligand electron transition. Fig. 4a. The UV spectrum of theoretical TD-DFT/B3LYP in gaseous state revealed one broad signal with λ_{max} = 305 nm (Fig. 4b).
An acceptable matching between the theoretical TD-DFT/B3LYP and the experimental UV was recorded, and perhaps the extra maxima and the slightly shift in absorption maxima which were observed only in the experimental can be attributed to solvent-solute interaction effect [14, 15].

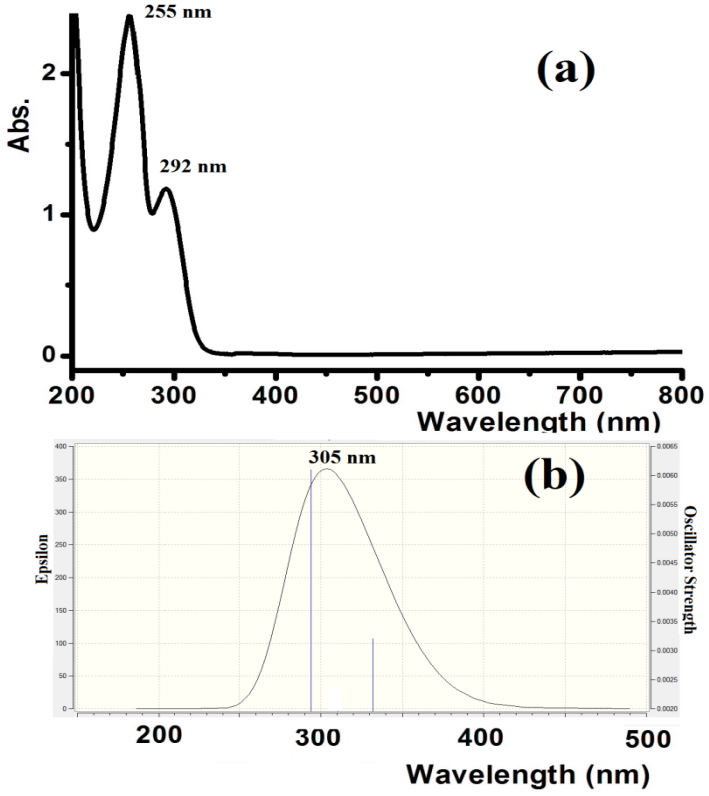

Fig. 4. (a) Experimental UV-visible spectrum of desired S.B in methanol λ_{max} = 255 and 292 nm and (b) theoretical TD-DFT/B3LYP 6-31G(d) in gaseous state with λ_{max} = 305 nm.

HOMO/LUMO of E-isomer of S.B.

Several chemical parameters can be calculated from HOMO/LUMO energy level like: electrophilicity, hardness, chemical potential, symmetry, quantum chemistry terms and electronegativity [27].
Fig. 5 illustrated the orbitals shapes and the energy levels of the HOMO/LUMO of *E*-isomer belong to the desired S.B in gaseous phase calculated. In HOMO piperazine ring gained the total electrostatic loops around, while in LUMO thiophene ring have the total loops intensity. HOMO and LUMO gap is related to the chemical reactivity or kinetic stability, since HOMO and LUMO have negative values that resolved a chemical stability of the desired S.B. [14, 15].

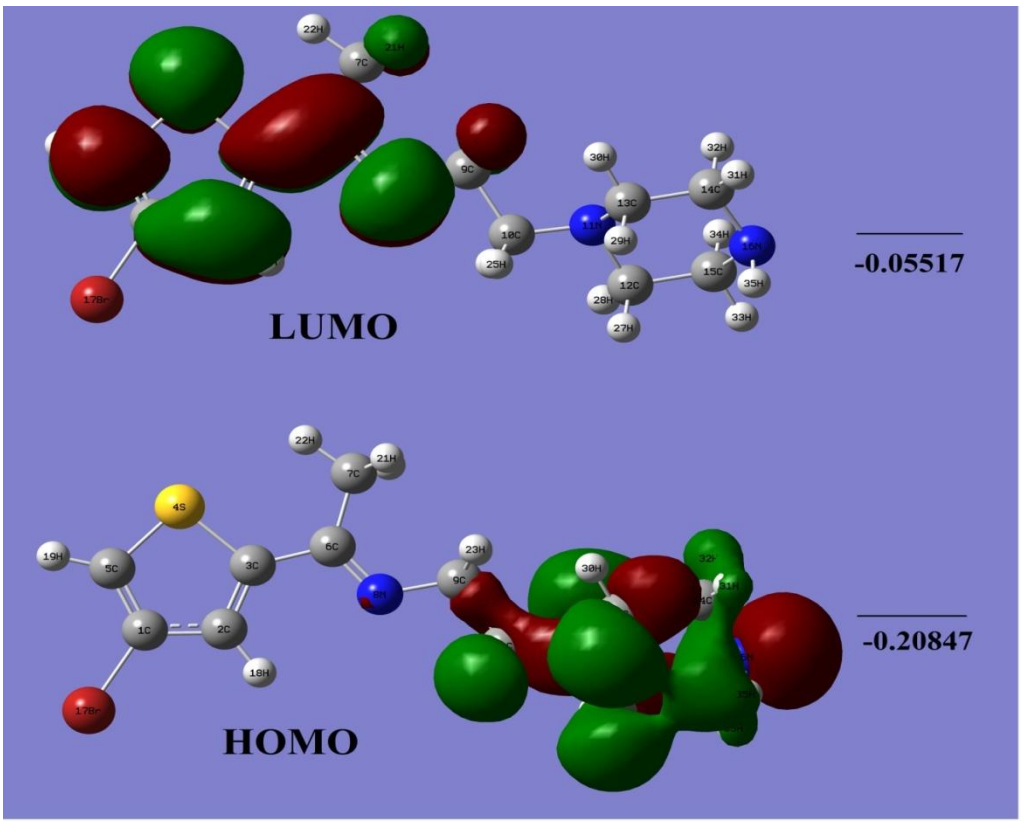

Fig. 5. HOMO/LUMO of *E*-isomer

GRD quantum parameters

The GRD of the desired molecule like electrophilicity (ω), hardness (η) electronegativity (χ), chemical potential (μ), and softness (σ) indices are helpful quantum parameters and were calculated from HOMO/LUMO energy gap using Koopman's notation (Table 6).

Electronegativity (χ) = $-E_{HOMO} + -E_{LUMO}$ /2

Hardness (η) = $E_{LUMO} - E_{HOMO}$ /2

Softness (σ) = 1/ η

Chemical potential (μ) = $-\chi$

Electrophilicity (ω) = μ^2/ 2η

Table 6. DFT/B3LYP/6-31G(d) calculated GRD quantum parameters of *E*-isomer of S.B.

	DFT/B3LYP/6-31G(d)
E_{HOMO}(eV)	-5.6727603
E_{LUMO}(eV)	-1.5012529
ΔE(eV)	4.17151
***X*(eV)**	3.58698
η(eV)	3.87924
σ(eV)	0.257732
μ(eV)	-3.58698
ω(eV)	1.658063

The value of the chemical potential revealed the non-spontaneous decomposition of such ligands. The hardness of the molecule revealed the polarizability reflected the fastness of electrons movement in molecules, the electrons donation and withdrawing ability power is indicated by its electronegativity and electrophilicity. Since the electronegativity is higher that its electrophilicity, this reflected the degree of electrons donation of such material and supported it as an excellent polydentate ligand.

MEP of E-isomer

The MEP is useful to evaluate the electrophilic and nucleophilic sites depending on the polarity of the functional groups of molecule. To do so, MEP/B3LYP for *E*-isomer of the S.B was evaluated, as shown in Fig. 6. The electrostatic potential are illustrated by different colors, the values of the electrostatic decreased in the order of red>orange> yellow>green>blue. The N atoms distinguished by red color as the most negative, the deepest in the red color among the three N atoms is the N of 2^o amine (N-H). Br is characterized with light orange, the blue color reflected the lowest in negative, the H of the 2^o amine, CH_3 and CH of thiophine are characterized by this color. The S and C-H aliphatic functional groups were characterized by the green color.

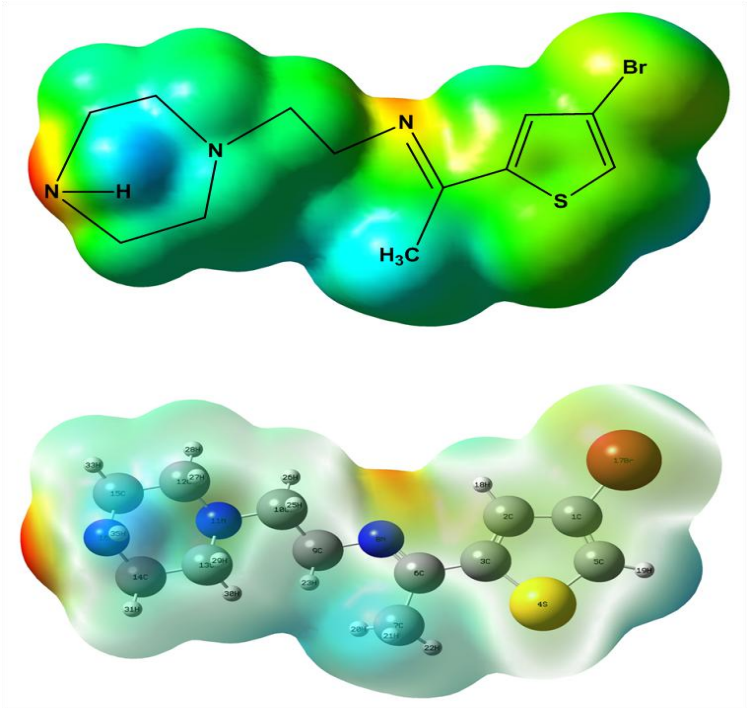

Fig. 6. MPE surface of E-isomer

Charge population (Mulliken atomic) analysis

Mulliken population charge calculation of the S.B was carried out by using B3LYP/6-31G(d) level of theory, Mulliken atomic charge distribution of acceptor and donor atoms in the desired S.B compound defined be +ve and –ve values, respectively, as seen in Table 7 and Fig. 7.

Table 7. *Mulliken atomic charge*

Atom No.	Atom Type	DFT	Atom No.	Atom Type	DFT
1	C	0.08089	18	H	0.179377
2	C	-0.12037	19	H	0.19465
3	C	-0.16911	20	H	0.183751
4	S	0.253284	21	H	0.18419
5	C	-0.35155	22	H	0.176226
6	C	0.300598	23	H	0.145695
7	C	-0.54849	24	H	0.169103
8	N	-0.43144	25	H	0.12161
9	C	-0.17549	26	H	0.153488
10	C	-0.1021	27	H	0.108556
11	N	-0.4117	28	H	0.138757
12	C	-0.127	29	H	0.106908
13	C	-0.14192	30	H	0.142392
14	C	-0.15123	31	H	0.139477
15	C	-0.15291	32	H	0.155846
16	N	-0.53701	33	H	0.14104
17	Br	-0.10063	34	H	0.156514
			35	H	0.288593

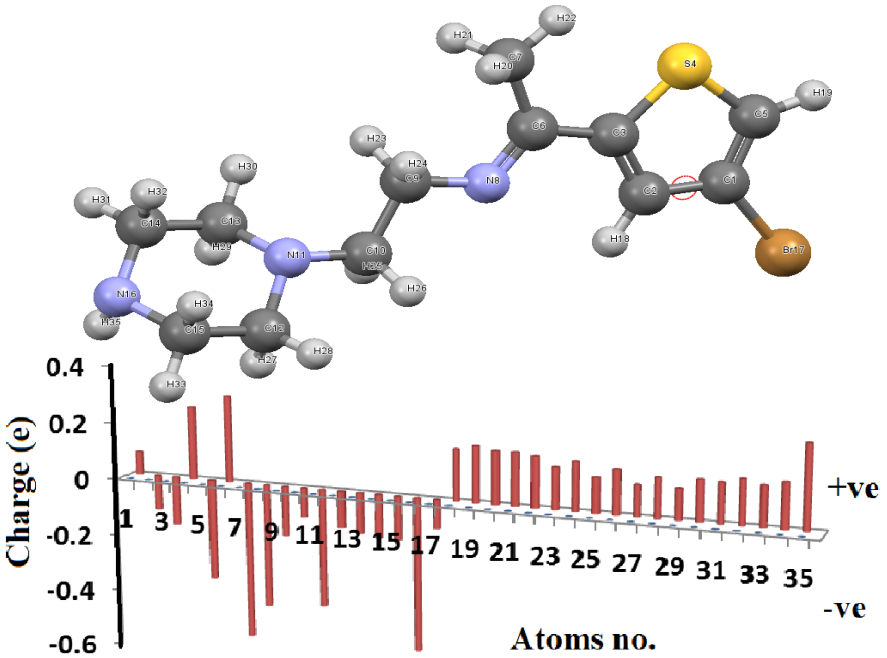

Fig. 7. DFT/B3LYP/6-31G(d) Mulliken charge distribution (per atom) of S.B.

The atomic charges were affected by several parameters like dipole moment, polarizability and refractivity [14]. The analysis revealed the presence of electrophilic and nucleophilic atoms in the backbone of the S.B. *Nucleophilic,* C7 (CH_3) reveled the highest nucleophilic behavior among all the atoms in the molecule with -0.55e, the three N atoms have also process high nucleophilicity ranging ~ -0.41e to -0.54e, the N of 2^o amine (N-H) found to be the highest in nucleophilicity among the three N atoms with -0.54e, Br reflected the poorest nucleophilic behavior among all the atoms with 0.10e. *Electrophilic*, C6 (imide carbon), H of 2^o amine (N-H), S in thiophene ring reflected the highest electrophilic atoms in the molecule with 0.35, 0.29 and 0.25e values, respectively. All the H atoms revealed electrophilic sites between 0.11−0.29e. Mulliken population charge data is consistent with the MPE map result.

Conclusion

N-(1-(4-bromothiophen-2-yl)ethylidene)-2-(piperazin-1-yl)ethanamine as a novel Schiff base ligand was made available in a very good yield. Several spectral analyses were performed to figure out the structural formula of the ligand. QM calculations for the desired compound like: TD-SCF, MPE, IR-vibration, NMR, Mulliken population were performed. DFT/B3LYP optimization showed that the more preferable isomer in gaseous state is *E*-isomer with a very small rotational energy. The theoretical calculations of the desired compound reflected a high degree of matching with their experimental coordinates parameters.

References

1. Juan A., Yaricruz P., Alina B., Juan, C., *Med. Chem.* 6 (2016) 467–473.
2. Pradhan R., Banik M., Cordes D., Slawin A., Sah N., *Inorg. Chimica Acta* 442 (2016) 70-75.
3. Gennari M., Pecaut J., Collomb M.N., Duboc C., *Dalton Trans.* 41 (2012) 3130-3134.
4. Ummer M.R., Dharmasivam M., Azees K.H., Rakesh P.N., Mukesh D., Aziz K.R., *New J. Chem.* 40 (2016) 2451–2465.
5. Petrus M.L., Bouwer R.K.M., Lafont U., Athanasopoulos S., Greenham N.C., Dingemans T.J., *J. Mater. Chem.* A 2 (2014) 9474-9480.
6. Prabhu J., Velmurugan K., Zhang Q., Radhakrishnan S., Tang L., Nandhakumar R., *J. Photochem. Photobio. A: Chem.* 337 (2017) 6–18.
7. Low M.L., Paulus G., Dorlet P., Guillot R., Rosli R., Delsuc N., Crouse K.A., Policar, C., *Biometals* 28 (2015) 553-560.
8. Shuvaev K.V., Dawe L.N., Thompson L.K., *Eur. J. Inorg. Chem.* 29 (2010) 4583–4586.

9. Bensaber S.M., Allafe H.a., Ermeli N.B., Mohamed S.B., Zetrini A., Alsabri S. G., Erhuma M., Hermann A., Jaeda M.I., Gbaj A.M., *Med. Chem*. 23 (2014) 5120-5130.
10. Chandramouli C., Shivanand M.R., Nayanbhai T.B., Bheemachari B., Udupi R.H., *J. Chem. Pharm. Res.* 4 (2012) 151–1159.
11. Liang C., Xia J., Lei D., Li X., Yao Q., Gao J., *Eur. J. Med. Chem.* 74 (2014) 742-750
12. Singh A.K., Pandey S.K., Pandey O.P., Sengupta S.K., *J. Mol. Struct*. 1074 (2014) 376-382.
13. Sunitha M., Padmaja M., Anupama B., Gyana Kumari C., *J. Fluorescence* 22 (2012) 1003–1012.
14. Warad I., Al-Demeri Y., Al-Nuri M., Shahwan S., Abdoh M., Naveen Sh., Lokanath N. K., Mubarak M. S., Hadda T. B., Mabkhot Y. N., *J. Mol. Struct.* 1142, (2017), 217–225.
15. Barakat A., Soliman S. M., Ghabbour H. A., Ali M., Al-Majid A. M., Zarrouk A., Warad I., *J. Mol. Struct*., 1137 (2017) 354–361.
16. Barakat A., Al-Majid A. M., Islam M. Sh., Warad I., Masand V. H., Yousuf S., Choudhary M. I. *Res. Chem. Intermed.* 42 (2016) 4041–4053.
17. Warad I., Azam M., Al-Resayes S. I., Shahidu M., Sarfaraz I., Salim A., Haddad F., *Res. Chem. Intermed.* 42 (2016) 379–389.
18. Warad I., Al-Demeri Y., Al-Nuri M., Suleiman M., Al-Ali A., Amereih S., *Molbank* (2016), M903.
19. Janim A., Al-Nuri M., Bani Odeh A., Barghouthi S. A., Ayesh M., Al Ali A., Amereih S., Warad I., *J. Mater. Environ. Sci.* 7 (2016) 3447-3453
20. Al-Noaimi M., Choudhar M., Awwadi F., Talib W., Hadda T. B., Yousuf S., Sawafta A., Warad I., *Spectrochimica Acta Part A.*, 127 (2015) 225-232.
21. Azam M.; Warad I.; Al-Resayes S.; Aldzaqr N.; Kha M.; Pallepogu R.; Dwivedi S.; Musarrat J.; Shaki M. *J. Mol. Struct.* 1047 (2013) 48–54.
22. Warad I., Al-Rimawi F., Barakat A., Affouneh S., Shivalingegowda N., Lokanath N. K., Abu-Reidah I. M., *Chem. Cen. J.* 10 (2016) 11-21.
23. Warad I., Barakat A., *J. Molec. Strut*. 1134 (2017) 17-24.
24. Banfi D., Patiny L., *CHIMIA* 62 (2008) 280-283.
25. Fukui K., *Science* 218 (1982) 747-750.
26.Aihara J., *J. Phys. Chem.* A 103 (1999) 7487-7493.
27. Singh A.K., Pandey S.K., Pandey O.P., Sengupta S.K., *J. Mol. Struct.* 1074 (2014) 376-382.
28. Frisch M.J., et al. GAUSSIAN 09, Revision B.09, GAUSSIAN, Inc., Pittsburgh, PA, 2009.

(2017) ; http://www.jmaterenvironsci.com